

Relativistic effects cannot explain galactic dynamics

L. Filipe O. Costa* and José Natário†

CAMGSD, Departamento de Matemática, Instituto Superior Técnico, 1049-001 Lisboa, Portugal

(Dated: September 20, 2024)

It has been suggested in recent literature that nonlinear and/or gravitomagnetic general relativistic effects can play a leading role in galactic dynamics, partially or totally replacing dark matter. Using the 1+3 “quasi-Maxwell” formalism, we show, on general grounds, such hypothesis to be impossible.

CONTENTS

I. Introduction	1
II. Equations of motion for massive particles and light in a stationary field	1
A. Geodesic equation in the “quasi-Maxwell” formalism	2
1. Timelike geodesics	2
2. Null geodesics	2
3. Timelike circular geodesics	3
B. Field equations	3
III. Gravitomagnetism cannot be the culprit—gravitational lensing	3
IV. Nonlinear GR effects work <i>against</i> attraction	5
V. Relevant examples	5
A. Post-Newtonian theory	5
1. System of N point bodies	5
2. Self-gravitating disks	6
3. Lensing around a spinning body	6
B. The Balasin-Grumiller (BG) “galactic” model	7
C. Gravitomagnetic dipole model	8
VI. Conclusion	10
Acknowledgments	10
A. Lensing in the Schwarzschild and Kerr spacetimes	10
References	12

I. INTRODUCTION

In a recent number of works, based both on linearized theory [1, 2] and exact models [3–7], it has been asserted that general relativistic effects (namely, gravitomagnetic ones) can have a significant impact [1, 2, 5, 7], or even totally account for the galactic flat rotation curves [3, 4, 6]. In the framework of a weak field slow motion approximation, this has been shown to be impossible, and such claims addressed, in Refs. [8–10]. It has however been argued [3–5, 7] that it is still

possible in the exact theory, due to nonlinear effects not captured in linearized theory (and not manifest “locally” [3–5]). In support of these claims, the Balasin-Grumiller (BG) model [5–7], or variants of it [3, 4, 7], have been used. Such model has been recently debunked in our Ref. [11], where it was shown to actually consist of a static dust, held in place by unphysical singularities along the symmetry axis, and that what actually rotates in the model are the ill chosen reference observers. In the present paper we address the general problem: assuming only stationarity of the solution, we show that (i) gravitomagnetism cannot be a relevant driving force of galactic dynamics; (ii) nonlinear general relativistic effects cannot account for any amount of the needed dark matter.

Notation and conventions.—Greek letters $\alpha, \beta, \gamma, \dots$ denote 4D spacetime indices, running 0–3; Roman letters i, j, k, \dots are spatial indices, running 1–3; $\epsilon_{\alpha\beta\gamma\delta} \equiv \sqrt{-g}[\alpha\beta\gamma\delta]$ is the 4D Levi-Civita tensor, with the orientation $[1230] = 1$; $\epsilon_{ijk} \equiv \sqrt{h}[ijk]$ is the Levi-Civita tensor in a 3D Riemannian manifold Σ of metric h_{ij} . Arrow notation \vec{X} denotes spatial 3-vectors on Σ , with components X^i . Indices of spatial tensors on Σ are raised and lowered with h_{ij} : $X_i = h_{ij}X^j$. The basis vector corresponding to a coordinate ϕ is denoted by $\partial_\phi \equiv \partial/\partial\phi$, and its α -component by $\partial_\phi^\alpha \equiv \delta_\phi^\alpha$.

II. EQUATIONS OF MOTION FOR MASSIVE PARTICLES AND LIGHT IN A STATIONARY FIELD

The line element $ds^2 = g_{\alpha\beta}dx^\alpha dx^\beta$ of a stationary spacetime can generically be written as

$$ds^2 = -e^{2\Phi}(dt - \mathcal{A}_i dx^i)^2 + h_{ij}dx^i dx^j, \quad (1)$$

where $e^{2\Phi} = -g_{00}$, $\Phi \equiv \Phi(x^j)$, $\mathcal{A}_i \equiv \mathcal{A}_i(x^j) = -g_{0i}/g_{00}$, and $h_{ij}(x^k) = g_{ij} + e^{2\Phi}\mathcal{A}_i\mathcal{A}_j$. We are interested in the equations of motion with respect to the coordinate system in (1); it is thus useful to refer to quantities as measured by the observers at rest in such coordinates (“static” observers). These observers have 4-velocity $u^\alpha = e^{-\Phi}\partial_t^\alpha \equiv e^{-\Phi}\delta_0^\alpha$, and their worldlines are tangent to the timelike Killing vector field ∂_t . The quotient of the spacetime by their worldlines yields a 3D Riemannian manifold Σ with metric h_{ij} , which these observers regard as the “spatial metric”, since $dl = \sqrt{h_{ij}dx^i dx^j}$ yields the infinitesimal spatial distance between them as measured by Einstein’s light signaling procedure (e.g., by radar) [12]. The 3D metric h_{ij} is identified in spacetime with the *space projector* with respect to u^α , $h_{\alpha\beta} \equiv g_{\alpha\beta} + u_\alpha u_\beta$ (observe that $h_{0\alpha} = 0$).

* filipecosta@tecnico.ulisboa.pt

† jnatar@math.ist.utl.pt

As discussed in detail in [11], when the congruence of static observers is asymptotically inertial [which is the case when their acceleration and vorticity, Eq. (7) below, asymptotically vanish], the coordinate system in (1) has axes anchored to inertial frames at infinity, being a generalization of the International Astronomical Union reference system to the exact metric (1). Such reference frame is in practice realized setting it up fixed with respect to remote celestial objects (namely quasars), and it is with respect to such a frame that, for instance, galactic rotation curves are defined.

A. Geodesic equation in the “quasi-Maxwell” formalism

Let $x^\alpha(\lambda)$ be the geodesic worldline of a test particle (that can have zero mass) and λ an affine parameter along it. The space components of the geodesic equation $d^2x^\alpha/d\lambda^2 = -\Gamma_{\mu\nu}^\alpha(dx^\mu/d\lambda)(dx^\nu/d\lambda)$ can be written as¹

$$\frac{d^2x^i}{d\lambda^2} + \Gamma(h)_{jk}^i \frac{dx^j}{d\lambda} \frac{dx^k}{d\lambda} = \nu \left[\nu \vec{G} + \frac{d\vec{x}}{d\lambda} \times \vec{H} \right]^i \quad (2)$$

where $\nu \equiv -u_\alpha dx^\alpha/d\lambda$,

$$\Gamma(h)_{jk}^i \equiv \frac{1}{2} h^{il} (h_{lj,k} + h_{lk,j} - h_{jk,l}) \quad (3)$$

are the Christoffel symbols of the space metric h_{ij} , and

$$G_i = -\Phi_{,i}; \quad H^i = e^\Phi \epsilon^{ijk} \mathcal{A}_{k,j} \quad (\epsilon_{ijk} \equiv \sqrt{h} [ijk]) \quad (4)$$

are fields living on the space manifold Σ , dubbed, respectively, “gravitoelectric” and “gravitomagnetic” fields, for playing in Eq. (2) roles analogous to the electric and magnetic fields in the Lorentz force equation. For a 3-vector \vec{X} on Σ , one can define the 3D covariant derivative with respect to h_{ij}

$$\frac{\tilde{D}X^i}{d\lambda} \equiv \frac{dX^i}{d\lambda} + \Gamma(h)_{jk}^i X^j \frac{dx^k}{d\lambda}. \quad (5)$$

1. Timelike geodesics

For timelike worldlines, one can set $\lambda = \tau$, so $dx^\alpha/d\tau \equiv U^\alpha$ is the 4-velocity, $\nu = -u_\alpha U^\alpha \equiv \gamma$ becomes the Lorentz factor between U^α and u^α , and Eq. (2) can therefore be written as [12–17] (cf. also [18, 19]),

$$\frac{\tilde{D}\vec{U}}{d\tau} = \gamma \left[\gamma \vec{G} + \vec{U} \times \vec{H} \right] \quad (6)$$

where \vec{U} is the 3-vector of components $(\vec{U})^i = U^i$, tangent to the spatial curve $x^i(\tau)$ obtained by projecting the geodesic

onto Σ . Equation (6) describes the acceleration of such 3D projected curve [since the left-hand member of (2) is the standard 3D covariant acceleration]. Its physical interpretation is that, from the point of view of the static observers, the spatial trajectory of the test particle will appear accelerated, as if acted upon by fictitious forces (inertial forces), arising from the fact that the reference frame is *not inertial*. In fact, \vec{G} and \vec{H} are identified in spacetime, respectively, with minus the acceleration and twice the vorticity of the static observers:

$$G^\alpha = -\nabla_{\mathbf{u}} u^\alpha \equiv -u_{;\beta}^\alpha u^\beta; \quad H^\alpha = 2\omega^\alpha = \epsilon^{\alpha\beta\gamma\delta} u_{\gamma;\beta} u_\delta. \quad (7)$$

Here $\epsilon^{\alpha\beta\gamma\delta} = [\alpha\beta\gamma\delta]/\sqrt{-g}$ is the 4D contravariant Levi-Civita tensor, and in the correspondence with (4) it is useful to note that $-g = he^{2\Phi}$. Decomposing U^α in terms of its projections parallel and orthogonal to u^α ,

$$U^\alpha = \gamma(u^\alpha + v^\alpha); \quad \gamma \equiv -u^\alpha U_\alpha = \frac{1}{\sqrt{1 - v^\alpha v_\alpha}}, \quad (8)$$

where v^α is the spatial velocity of the particle relative to the static observers [11, 15, 18], Eq. (6) can be rewritten as

$$\frac{\tilde{D}\vec{U}}{d\tau} = \gamma^2 \left[\vec{G} + \vec{v} \times \vec{H} \right]. \quad (9)$$

2. Null geodesics

In the case of light rays (null geodesics), of tangent $k^\alpha = dx^\alpha/d\lambda$, Eqs. (2) and (5) analogously yield

$$\frac{\tilde{D}\vec{k}}{d\lambda} = \nu \left[\nu \vec{G} + \vec{k} \times \vec{H} \right]; \quad \nu \equiv -k^\alpha u_\alpha. \quad (10)$$

An equivalent formulation in terms of the photon’s null 4-momentum is given in [19], Eqs. (10.2)–(10.3), and a Lagrangian formulation in [20]. The null vector k^α decomposes, in terms of its projections parallel and orthogonal to u^α , as [21]

$$k^\alpha = \nu(u^\alpha + v^\alpha) \quad (11)$$

where v^α is a *unit* vector orthogonal to u^α , yielding the photon’s spatial velocity relative to u^α . Therefore, $\vec{k} = \nu\vec{v}$, and one can re-write (10) as

$$\frac{\tilde{D}\vec{k}}{d\lambda} = \nu^2 \left[\vec{G} + \vec{v} \times \vec{H} \right]. \quad (12)$$

Equations (10)–(12) tell us that, just like massive particles, light rays in a stationary spacetime behave analogously to charged particles under the action of an electric and magnetic fields [20]. A difference, however, is that the second term in the left-hand member of (2), which reads here $\Gamma(h)_{jm}^i k^j k^m$, is typically of the same order magnitude as the first term in (10) [contrary to the case of $\Gamma(h)_{jm}^i U^j U^m = O(v^2)$ for slowly moving massive particles].

¹ Using the Christoffel symbols $\Gamma_{00}^i = -e^{2\Phi} G^i$, $\Gamma_{j0}^i = e^{2\Phi} \mathcal{A}_j G^i - e^\Phi H_{j/2}^i$, and $\Gamma_{jk}^i = \Gamma(h)_{jk}^i - e^\Phi \mathcal{A}_{(k} H_{j)}^i - e^{2\Phi} G^i \mathcal{A}_j \mathcal{A}_k$, where $H_{ij} \equiv e^\Phi [\mathcal{A}_{j,i} - \mathcal{A}_{i,j}]$.

3. Timelike circular geodesics

In an axistationary spacetime we have $g_{0i}dx^i = g_{0\phi}d\phi$. If there is reflection symmetry about the equatorial plane [22], then $g_{\alpha\beta,z} = 0$ (or $g_{\alpha\beta,\theta} = 0$) along that plane; noticing that the geodesic equation can be written in the form (see e.g. [23]) $dU_\alpha/d\tau = g_{\mu\nu,\alpha}U^\mu U^\nu/2$, then $dU_z = 0$ therein, allowing equatorial geodesic motion. For circular equatorial geodesics, $U^\alpha = U^0(\delta_0^\alpha + \Omega_{\text{geo}}\delta_\phi^\alpha)$, where the angular velocity $\Omega_{\text{geo}} \equiv d\phi/dt = U^\phi/U^0$ is obtained from the r -component of the geodesic equation, $dU_r/d\tau = g_{\mu\nu,r}U^\mu U^\nu/2 = 0$:

$$\Omega_{\text{geo}\pm} = \frac{-g_{0\phi,r} \pm \sqrt{g_{0\phi,r}^2 - 2g_{\phi\phi,r}e^{2\Phi}G_r}}{g_{\phi\phi,r}}. \quad (13)$$

In the equatorial plane, given an arbitrary radial coordinate r , through the coordinate transformation $r_w(r) = e^{\Phi(r)}\sqrt{h_{\phi\phi}(r)}$, the metric can be written in the form (1) with $h_{\phi\phi} = e^{-2\Phi}r_w^2$. This is the case of the Weyl canonical coordinates (cf. e.g. Eq. (19.21) of [24]); it is also the case (to the accuracy at hand) of the radial coordinate $r = \sqrt{x^2 + y^2}$ associated to the post-Newtonian (PN) coordinate system in Eq. (20) below. It follows from (8) that the magnitude $\|v_{\text{geo}\pm}^\alpha\| = (1 - \gamma_{\text{geo}\pm}^{-2})^{1/2}$ of the velocity of the circular geodesics relative to the static observers $u^\alpha = e^{-\Phi}\delta_0^\alpha$ reads, in such coordinates, for $G_{r_w} \neq 0$,

$$\|v_{\text{geo}\pm}^\alpha\| = \frac{2r_w|G_{r_w}|}{|\sqrt{-g(H^z)^2 - 4r_w G_{r_w}(1 + r_w G_{r_w})} \pm \sqrt{-g}H^z|}. \quad (14)$$

where we have noted, from (4), that $\mathcal{A}_{\phi,r} = e^{-\Phi}\epsilon_{r\phi i}H^i = e^{-2\Phi}\sqrt{-g}H^z$.

B. Field equations

The fields \vec{G} and \vec{H} that govern the geodesic equation (2) obey [15]

$$\tilde{\nabla} \cdot \vec{G} = -4\pi(2\rho + T_\alpha^\alpha) + \vec{G}^2 + \frac{1}{2}\vec{H}^2; \quad \tilde{\nabla} \times \vec{G} = 0; \quad (15)$$

$$\tilde{\nabla} \cdot \vec{H} = -\vec{G} \cdot \vec{H}; \quad \tilde{\nabla} \times \vec{H} = -16\pi\vec{J} + 2\vec{G} \times \vec{H}, \quad (16)$$

where $\rho \equiv T^{\alpha\beta}u_\alpha u_\beta$ and $J^\alpha \equiv -T^{\alpha\beta}u_\beta$ are, respectively, the mass-energy density and current 4-vector as measured by the static observers of 4-velocity $u^\alpha = e^{-\Phi}\delta_0^\alpha$. Here $\tilde{\nabla}$ denotes covariant differentiation with respect to the spatial metric h_{ij} , with Christoffel symbols (3). The equations for $\tilde{\nabla} \cdot \vec{G}$ and $\tilde{\nabla} \times \vec{H}$ are, respectively, the time-time and time-space projections, with respect to u^α , of the Einstein field equations $R_{\alpha\beta} = 8\pi(T_{\alpha\beta} - \frac{1}{2}g_{\alpha\beta}T_\gamma^\gamma)$; the equations for $\tilde{\nabla} \cdot \vec{H}$ and $\tilde{\nabla} \times \vec{G}$ follow from (4).

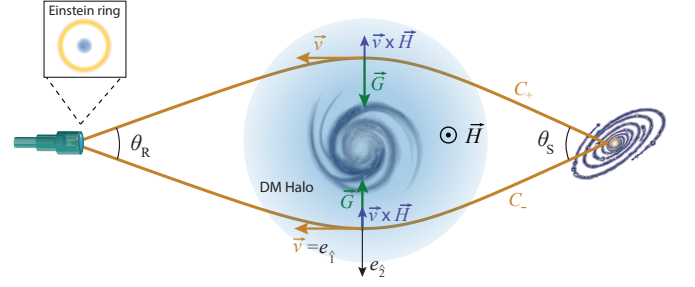


Figure 1. Gravitational lensing by galactic dark matter halos. When the observer, foreground, and emitting galaxies are aligned, an Einstein ring forms. Nearly perfect Einstein rings have been detected, such as in the system B1938+666, or the “Cosmic Horseshoe” J1148+1930. The majority of the lensing effect is estimated to come from dark matter. The gravitomagnetic field cannot mimic such effects, since the inertial force $\vec{v} \times \vec{H}$ does not contribute to make light rays converge in such setting; e.g., in the equatorial plane, it deflects photons on both sides of the body in the same direction (the effect being anyway negligible for any realistic galactic model).

III. GRAVITOMAGNETISM CANNOT BE THE CULPRIT—GRAVITATIONAL LENSING

Alongside the galactic rotation curves, there is a set of other effects consistently indicating hypothetical dark matter (DM) halos around galaxies. Any viable alternative to DM must explain these effects. One of the most compelling of such indications is the observed galactic gravitational lensing, which cannot be accounted for by visible baryonic matter alone. It is well known that, when the emitting object (light source), the foreground galaxy (lens), and the observer are nearly aligned (see Fig 1), roughly circular rings (Einstein rings [25–31]) are formed, as in the case of the system B1938+666 [27, 32, 33] (the first detected complete Einstein ring), or the “Cosmic Horseshoe” J1148+1930 [34–38]. The majority of the mass causing such lensing effect is estimated to consist of dark matter [33, 35–38], and is consistent with the halos’ shape being roughly spherical or moderately deformed (namely prolate [37], as seems to be more common [39]). Anomalies in such rings have actually been recently proposed [40] as a mean of determining the nature of dark matter, namely distinguishing between weakly interacting massive particles and axions.

These effects could not take place if the gravitomagnetic field \vec{H} were the main driver of galactic dynamics. For a rotating body, under the assumptions of stationarity and reflection symmetry about the equatorial plane, \vec{H} is axisymmetric, orthogonal to the equatorial plane, and pointing in the same direction along the whole plane. It follows from Eq. (12) that the gravitomagnetic “force” $\vec{v} \times \vec{H}$ on light rays passing through opposite sides of the body points in the same direction, thus not contributing to produce symmetric convergence of light rays along the line of sight of observers aligned with the light source and the foreground galaxy (setting illustrated in Fig. 1). This can be seen also using the Gauss-Bonnet theorem [41–47]: the light ray trajectories C_\pm illustrated in Fig. 1 are the projections of the photon’s null geodesics $C_\pm^{(4)}$ onto

the space manifold Σ , $\pi_\Sigma C_\pm^{(4)} = C_\pm$. Let \mathcal{S} be an oriented 2-surface on Σ bounded by C_\pm : $\partial\mathcal{S} = C_+ \cup (-C_-)$, where $-C_-$ is the curve with the opposite orientation of C_- . Then

$$\theta_R = \iint_{\mathcal{S}} K d\mathcal{S} + \int_{C_+} \kappa_g d\lambda - \int_{C_-} \kappa_g d\lambda - \theta_S - 2\pi[\chi(\mathcal{S}) - 1], \quad (17)$$

where K is the Gaussian curvature of \mathcal{S} and $\chi(\mathcal{S})$ its Euler characteristic [if simply connected, namely in the absence of singularities, $\chi(\mathcal{S}) = 1$], and κ_g is the geodesic curvature [41, 48, 49] of a curve C of tangent vector $\dot{C}(\lambda)$. Considering a positively oriented orthonormal frame $\{e_{\hat{1}}, e_{\hat{2}}\}$ on \mathcal{S} along C such that $e_{\hat{1}} = \dot{C}/\|\dot{C}\|$ (see Fig. 1), the geodesic curvature of C is given by [48]

$$\kappa_g = \frac{1}{\|\dot{C}\|} \langle \tilde{\nabla}_{\dot{C}} e_{\hat{1}}, e_{\hat{2}} \rangle = \frac{\langle \tilde{\nabla}_{\dot{C}} \dot{C}, e_{\hat{2}} \rangle}{\|\dot{C}\|^2},$$

where $\tilde{\nabla}$ is the Levi-Civita covariant derivative of² (Σ, h) , with Christoffel symbols (3), as defined above. For light rays, $\dot{C} = \vec{k}$, $\|\dot{C}\|^2 = h_{\alpha\beta} k^\alpha k^\beta = \nu^2$ [cf. Eq. (11)], and $e_{\hat{1}} = \vec{v}$. Recalling that the left-hand member of (2) is the 3D covariant acceleration $\tilde{\nabla}_{\dot{C}} \dot{C}$, by Eq. (12) we have $\tilde{\nabla}_{\dot{C}} \dot{C} = \nu^2[\vec{G} + \vec{v} \times \vec{H}]$; hence,

$$\kappa_g = \langle \vec{G}, e_{\hat{2}} \rangle + \langle \vec{v} \times \vec{H}, e_{\hat{2}} \rangle \equiv G^{\hat{2}} + (\vec{v} \times \vec{H})^{\hat{2}}. \quad (18)$$

For the setting in Fig. 1, in the equatorial plane, $(\vec{v}_\pm \times \vec{H})^{\hat{2}} = -\|\vec{H}\|$; hence, the gravitomagnetic contributions to the convergence angle θ_R in Eq. (17) have *opposite* signs. In particular, for the case where the rays are approximately symmetric, as required for a nearly perfect Einstein ring, we have, due to the reflection symmetry about the source-lens-observer axis, $\int_{C_+} \|\vec{H}\| d\lambda \approx \int_{C_-} \|\vec{H}\| d\lambda$ and $\int_{C_+} G^{\hat{2}} d\lambda \approx -\int_{C_-} G^{\hat{2}} d\lambda$; therefore,

$$\int_{C_+} \kappa_g d\lambda - \int_{C_-} \kappa_g d\lambda \approx 2 \int_{C_+} G^{\hat{2}} d\lambda,$$

so the gravitomagnetic force does not contribute to θ_R in Eq. (17). Indeed, the effect of the gravitomagnetic force would be to cause the light rays that reach an observer aligned with the source and foreground galaxy to arrive at different angles from each side, as exemplified in Appendix A for the case of a Kerr black hole. Moreover, in the far field regime, the gravitomagnetic field of a galaxy (as for any spinning body) is dipole-like,

² In earlier works [41, 44, 46] on gravitational lensing from the Gauss-Bonnet theorem, to the same underlying quotient manifold Σ , a different Riemannian metric $\gamma_{ij} = e^{-2\Phi} h_{ij}$ (“generalized optical” metric [41]) is associated. The motivation being that, in the static case $\mathcal{A}_t = 0$, γ_{ij} yields an optical metric [44] (“Fermat” metric [46]), in the sense that the projection $C = \pi_\Sigma C^{(4)}$ of null geodesics $C^{(4)}$ onto Σ yields geodesics with respect to the metric γ_{ij} . The two approaches are equivalent, working with h_{ij} being more suitable for our purposes, by making explicit the role of the inertial fields \vec{G} and \vec{H} .

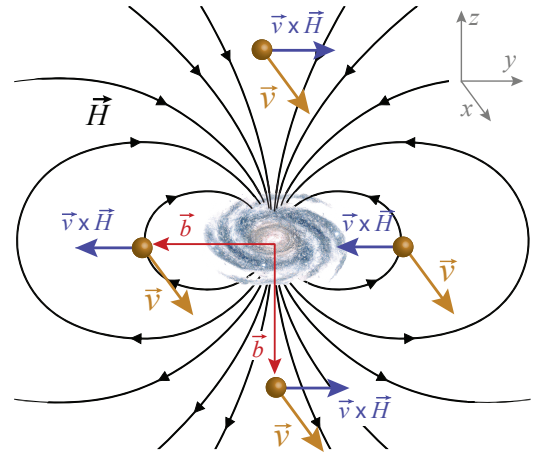


Figure 2. Gravitomagnetic field \vec{H} produced by a galactic disk. At large distances, it is dipole-like, deflecting photons with impact parameter \vec{b} orthogonal to the equatorial plane in a direction opposite to those for which \vec{b} lies in the equatorial plane (in both cases, photons through opposite sides of the body being deflected in the same direction); this produces no convergence of light rays along the line of sight of observers aligned with the light source and the foreground galaxy.

as illustrated in Fig. 2; hence, light rays with impact parameter \vec{b} orthogonal to the equatorial plane are deflected in a direction parallel to that plane (thus orthogonal to \vec{b}), which again produces no convergence, cf. Secs. VA3 and Appendix A. As a consequence, not only \vec{H} does not contribute, as it acts against the formation of Einstein rings (actually precluding them for small light sources). This is well known in the case of the Kerr spacetime [20, 50–52], discussed in Appendix A, and for generic rotating sources in the weak field limit [53], discussed in Sec. VA3 below. This is in spite of, for astrophysical lenses, \vec{H} (thus $\vec{v} \times \vec{H}$) being smaller (typically much smaller) than \vec{G} along the light ray’s path.

Observe now the crucial difference in magnitude (for a given \vec{H}) between the gravitomagnetic forces $\vec{v} \times \vec{H}$ on light and on massive astrophysical bodies,

$$\text{photons : } v = 1 \Rightarrow |\vec{v} \times \vec{H}| \sim |\vec{H}|$$

$$\text{stars in galaxy : } v \lesssim 10^{-3} \Rightarrow |\vec{v} \times \vec{H}| \lesssim 10^{-3} |\vec{H}|.$$

By Eq. (9), in order for $\vec{v} \times \vec{H}$ to have a relevant impact on the galactic rotation curves, one would need $|\vec{H}| \gtrsim 10^3 |\vec{G}|$. Such a gravitomagnetic field (impossible for a physical source, cf. Sec. VA3) would yield a gravitational lens with a gravitomagnetic force three orders of magnitude larger than the gravitoelectric term: $|\vec{v} \times \vec{H}| \sim |\vec{H}| \gtrsim 10^3 |\vec{G}|$ (thus than the Newtonian contribution). This, besides precluding Einstein rings, would produce bending angles much larger than observed, as can be checked using the Gauss-Bonnet theorem (employing it, with κ_g as given in Eq. (18) above, to the quadrilateral in e.g. Fig. 2 of [41]; cf. also Eq. (30) therein), or, in linearized theory, using Eq. (28) below, leading to extreme lensing effects also very different from those observed. This is a trait

common to the ‘‘galactic’’ models based on gravitomagnetism proposed in the literature, as exemplified in Secs. V A 3 and V B below.

IV. NONLINEAR GR EFFECTS WORK AGAINST ATTRACTION

The analysis in the previous section shows that not only the gravitomagnetic field \vec{H} cannot replace the role of dark matter in gravitational lensing, as the observed deflection angles constrain \vec{H} in galaxies to be, at most, within the order of magnitude of \vec{G} (actually having to be considerably smaller, in order to allow for the Einstein rings). For the motion of stars, since $v \lesssim 10^{-3}$, this effectively renders the gravitomagnetic term $\vec{v} \times \vec{H}$ in Eq. (9) irrelevant compared to the gravitoelectric term. The measured star velocities constrain likewise the magnitude of \vec{G} to $|\vec{G}|r \sim v^2 \lesssim 10^{-6}$; from (14), we have thus, for the velocity of the circular equatorial geodesics,

$$\|v_{\text{geo}\pm}^\alpha\| = \sqrt{r_w G_{r_w}} + O(10^{-9}; 10^{-6} |\vec{H}|/|\vec{G}|), \quad (19)$$

which is ruled by G^α , as expected (and formally similar to the Keplerian law). We stress that the approximate expression (19) follows merely from observational constraints, not linearized theory; indeed \vec{G} , so far, remains a nonlinear field. The same conclusion³ can be reached from the angular velocity (13), which yields $\Omega_{\text{geo}\pm} = e^\Phi (-2G_r/g_{\phi\phi,r})^{1/2} (1 + [\text{terms} < 10^{-3}])$ (where one can take $g_{\phi\phi} = r^2$, since it is also well known from experiment that the galactic space metric is very weakly curved).

Thus it remains only to clarify whether nonlinear GR effects can amplify \vec{G} in order to produce an attractive effect able to sustain the rotation curves. It is clear however, from the first of Eqs. (15), that the nonlinear terms \vec{G}^2 and $\vec{H}^2/2$ act as effective negative ‘‘energy’’ sources for \vec{G} [13], countering the attractive effect of the source term $2\rho + T_\alpha^\alpha (= \rho$ for dust). Hence, they only *aggravate* the need for dark matter. This is manifest already in post-Newtonian (PN) theory, see Sec. V A below. It is also clear, based on PN theory, that the effect is anyway negligible in any realistic galactic model, given the weakness of the galactic gravitational field (cf. Secs. V A 1 and V A 2). It is huge, however, in some galactic models proposed in the literature. Namely, in the Balasin-Grumiller dust model (Sec. V B below), the effect is such that it completely kills off the attractive contribution from the dust’s mass density ρ , yielding $\vec{G} = 0$ [11].

³ As discussed in Sec. III F of [11], rotation curves are a notion of Newtonian and post-Newtonian theories, whose generalization to exact GR is not unambiguous. The angular velocity (13) and the relative velocity (14) are two precise notions, both yielding the usual rotation curve in the Newtonian limit, but which are however distinct (one being an angular velocity with respect to coordinate time t , the other a velocity with respect to the static observers, hence to their proper time τ , obeying $d\tau = \sqrt{-g_{00}dt}$).

V. RELEVANT EXAMPLES

A. Post-Newtonian theory

In the post-Newtonian (PN) expansion of general relativity, at first (1PN) order, the metric can be written, in geometrized units, as [54–56]

$$\begin{aligned} g_{00} &= -1 + 2w - 2w^2 + O(6); \\ g_{i0} &= \mathcal{A}_i + O(5); \quad g_{ij} = \delta_{ij} (1 + 2w) + O(4), \end{aligned} \quad (20)$$

where $O(n) \equiv O(\epsilon^n)$, ϵ is a small *dimensionless* parameter such that $U \sim \epsilon^2$, U is minus the Newtonian potential, and $w = U + O(4)$ consists of the sum of the Newtonian potential U plus *nonlinear* terms of order ϵ^4 . The bodies’ velocities are assumed such that $v \lesssim \epsilon$ (since, for bounded orbits, $v \sim \sqrt{U}$), and time derivatives increase the degree of smallness of a quantity by a factor ϵ ; for example, $\partial U/\partial t \sim Uv \sim \epsilon U$. The geodesic equation for a test particle can be written as [54]

$$\frac{d^2 \vec{x}}{dt^2} = (1 + v^2 - 2U)\vec{G} + \vec{v} \times \vec{H} - 3 \frac{\partial U}{\partial t} \vec{v} - 4(\vec{G} \cdot \vec{v})\vec{v} + O(6) \quad (21)$$

with

$$\vec{G} = \nabla w - \frac{\partial \vec{\mathcal{A}}}{\partial t} + O(6); \quad \vec{H} = \nabla \times \vec{\mathcal{A}} + O(5). \quad (22)$$

In the stationary case (i.e., neglecting all time derivatives), Eq. (21) yields the post-Newtonian limit of Eq. (6), as can be seen noting that $\vec{D}\vec{U}/d\tau = (U^0)^2 d^2 \vec{x}/dt^2 - v^2 \vec{G} + 4(\vec{G} \cdot \vec{v})\vec{v} + O(6)$ and $(U^0)^{-2} = 1 - v^2 - 2U + O(4)$.

1. System of N point bodies

For a system of N gravitationally interacting point particles, the metric potentials read, in the *harmonic gauge* (e.g. [54, 56–58]),

$$\begin{aligned} w &= \sum_a \frac{M_a}{r_a} \left(1 + 2v_a^2 - \sum_{b \neq a} \frac{M_b}{r_{ab}} - \frac{1}{2} \vec{r}_a \cdot \vec{a}_a - \frac{(\vec{r}_a \cdot \vec{v}_a)^2}{2r_a^2} \right) \\ \vec{\mathcal{A}} &= -4 \sum_a \frac{M_a}{r_a} \vec{v}_a; \quad U = \sum_a \frac{M_a}{r_a}, \end{aligned} \quad (23)$$

where M_a is the mass of particle ‘‘a’’, $\vec{r}_a \equiv \vec{x} - \vec{x}_a$, \vec{x} is the point of observation, \vec{x}_a is the instantaneous position of particle ‘‘a’’, $\vec{v}_a = \partial \vec{x}_a/\partial t$ its velocity, $\vec{a}_a = \partial \vec{v}_a/\partial t$ its *coordinate* acceleration, and $\vec{r}_{ab} \equiv \vec{x}_a - \vec{x}_b$. The gravitoelectric and

gravitomagnetic fields (22) read

$$\begin{aligned} \vec{G} = & - \sum_a \frac{M_a}{r_a^3} \vec{r}_a \left[1 - 2 \sum_b \frac{M_b}{r_b} - \sum_{b \neq a} \frac{M_b}{r_{ab}} \right. \\ & \left. + 2v_a^2 - \frac{3(\vec{r}_a \cdot \vec{v}_a)^2}{2r_a^2} - \frac{1}{2}(\vec{r}_a \cdot \vec{a}_a) \right] \\ & + 3 \sum_a \frac{M_a}{r_a^3} (\vec{r}_a \cdot \vec{v}_a) \vec{v}_a + \frac{7}{2} \sum_a M_a \frac{\vec{a}_a}{r_a}; \end{aligned} \quad (24)$$

$$\vec{H} = -4 \frac{M_a}{r_a^3} \sum_a \vec{v}_a \times \vec{r}_a. \quad (25)$$

In the case of a single body at rest, the potentials (23) reduce to $w = M/r$, $\vec{A} = 0$, and (20) yields the 1PN limit of the Schwarzschild metric in isotropic or harmonic coordinates (obtained, to the accuracy at hand, from the usual Schwarzschild coordinates $\{t, \varrho, \theta, \phi\}$ through the substitution $\varrho = r + M$; cf., e.g., [58], pp. 268-270). Equations (24)-(25) yield in this case $\vec{H} = 0$ and

$$\vec{G} = -\frac{M}{r^3} \left(1 - \frac{2M}{r} \right) \vec{r}.$$

This is smaller than the Newtonian (OPN) gravitoelectric field $\vec{G}_N = -\vec{r}M/r^3$, showing that the nonlinear contribution *decreases* the gravitational attraction. The angular velocity of circular geodesics, Eq. (13), is

$$\Omega_{\text{geo}\pm} = \pm \left[\sqrt{\frac{M}{r^3}} - \frac{3}{2} \sqrt{\frac{M^3}{r^5}} \right],$$

which, accordingly, is *slower* than the Newtonian angular velocity $\Omega_N = \pm M^{1/2}/r^{3/2}$.

Stars in a galaxy can be considered, to a good approximation, point masses. In the Milky Way their velocities are of the order $v_a \sim 10^{-3}$, and their coordinate acceleration a_a of the order $v_a^2/r \sim 10^{-6}/r$; hence, the velocity and acceleration dependent terms in (24) are smaller by a 10^6 factor compared to the Newtonian term $\vec{G}_N = -\sum_a M_a \vec{r}_a/r_a^3$. The same applies to the velocity dependent terms in (21), by Eqs. (23)–(25). The remaining relativistic corrections are the nonlinear terms in the first line of Eq. (24) (which are negative, thus decreasing the magnitude of \vec{G}), plus the negative term $-2U\vec{G}$ in (21); all of them *decrease* the attraction, thus working against the sought effect for explaining the galactic rotation curves (the corrections being anyway negligible, comparing to the Newtonian terms).

2. Self-gravitating disks

The gravitational field of self-gravitating stationary fluids is described, to first post-Newtonian order, by the metric (20) with $w = U$ [59, 60]. The relativistic Euler equations are integrable provided that the angular momentum per unit mass j depends only on the angular velocity Ω [59]. A function $j(\Omega)$,

appropriate for toroids (including thin hollow disks, case that could represent a disk galaxy), is given in Eq. (8) of [59], leading to the rotation curve

$$\Omega = \Omega_N \left[1 - \frac{2}{1-\delta} \Omega_N^2 r^2 - \frac{4h_N}{1-\delta} \right] - \frac{\mathcal{A}_\phi}{r^2(1-\delta)} \quad (26)$$

(cf. Eq. (18) of [59]), where Ω_N is the Newtonian result, $\delta \in [-\infty, 0] \setminus \{-1\}$ is a parameter, and h_N the specific enthalpy at Newtonian (OPN) accuracy. The nonlinear contribution in the second term, again, *slows down* the rotation. This contribution, as well as the third and fourth terms of Eq. (26), are anyway negligible for the Milky Way: $\Omega_N^2 r^2 \sim 10^{-6} \gtrsim h_N$; and \mathcal{A}_ϕ , from its definition in e.g. Eqs. (8.4) of [58], is of order $\mathcal{A}_\phi/r^2 \sim 10^{-3}U/r \sim 10^{-6}\Omega_N$ (in agreement with the conclusion in [8]).

3. Lensing around a spinning body

The gravitational field of any isolated stationary matter distribution is described, to linear order, by the metric

$$ds^2 = (-1+2U)dt^2 + 2\mathcal{A}_i dx^i + \delta_{ij} (1+2U) dx^i dx^j, \quad (27)$$

which follows from linearizing (20) (cf. e.g. Eq. (27.32) of [61]). Consider light rays from a distant light source, at impact parameter \vec{b} , being scattered by the distribution (see e.g. Fig. 1 of [62]). Let \vec{v} be a unit vector parallel to the ray's direction [i.e., the photon's spatial velocity, as defined in Eq. (11)]. The change in the ray's direction, $\Delta\vec{v} = \vec{v}_f - \vec{v}_{in}$, is given by [28, 63] (cf. also [62])

$$\Delta\vec{v} = 2 \int_{-\infty}^{\infty} \vec{G} dt + \Delta\vec{v}_H; \quad \Delta\vec{v}_H = \int_{-\infty}^{\infty} \vec{v} \times \vec{H} dt, \quad (28)$$

where $\vec{G} = \nabla U$ and $\Delta\vec{v}_H$ is the gravitomagnetic deflection. The gravitomagnetic vector potential of the distribution is $\vec{A} = 2\vec{r} \times \vec{S}/r^3$, where \vec{S} is the angular momentum. Notice that this is a dipole-type potential, of dipole moment $-2\vec{S}$. The corresponding gravitomagnetic field is [cf. Eqs. (22)] $\vec{H} = 2\vec{S}/r^3 - 6(\vec{S} \cdot \vec{r})\vec{r}/r^5$, formally identical to the magnetic field of a magnetic dipole of moment $\vec{\mu} = -2\vec{S}$, as is well known (e.g. [64]). Equations (28) yield in this case [62, 65]

$$\Delta\vec{v}_H = \frac{4}{b^2} \left[\frac{2}{b^2} (\vec{b} \cdot (\vec{v}_{in} \times \vec{S}) \vec{b} - (\vec{v}_{in} \times \vec{S})) \right].$$

For pairs of light rays at opposite impact parameters $\pm\vec{b}$ (see Fig. 2), $\Delta\vec{v}_H$ is the same, thus not contributing to produce convergence. For \vec{v}_{in} and \vec{b} mutually orthogonal and lying in the equatorial plane (e.g. $\vec{v}_{in} = \|\vec{v}_{in}\| \vec{e}_x$, $\vec{b} = \pm\|\vec{b}\| \vec{e}_y$, $\vec{S} = \|\vec{S}\| \vec{e}_z$, as depicted in Fig. 2), the photons are deflected in the direction $\hat{v}_{in} \times \hat{S} (= -\vec{e}_y$, in Fig. 2) along the equatorial plane; for the same \vec{v}_{in} , but now \vec{b} orthogonal to the equatorial plane ($\vec{b} \parallel \pm\vec{S}$), the photons are again deflected parallel to the equatorial plane, but now in the opposite direction $-\hat{v}_{in} \times \hat{S}$.

Considering the Newtonian potential of a spherical source, $U = M/r$, and $0 \leq S/M^2 < 1$, Eq. (27) yields the linearized Kerr metric. It produces weak lensing images very similar to those displayed for the exact metric in Figs. (8)(c)–(d). Namely, for large enough light sources (see Appendix A), the lens acts like a shifted non-spinning lens [66, 67]. For extended objects (like fast-spinning stars) larger values of S/M^2 are possible; but still the gravitomagnetic field \vec{H} along the ray’s trajectory is smaller than (or, at best, when grazing the object, within the order of magnitude of) \vec{G} , since $S \lesssim Mv_{\text{rot}}R$ (where R is the body’s radius and v_{rot} its rotational velocity), and so in the body’s exterior $|\vec{H}|/|\vec{G}| \sim v_{\text{rot}}R/r < 1$, with $R/r < 1$ and $v_{\text{rot}} < 1$.

To entertain the possibility of \vec{H} having an impact on the galactic rotation curves, however, a much larger field would need to be considered, as discussed in Sec. III. According to Eq. (9), one would need $|\vec{H}| \gtrsim 10^3|\vec{G}|$ since, for stars in a galaxy, $v \lesssim 10^{-3}$. Besides impossible for a rotating body, as shown above, such \vec{H} would, by Eq. (28) (since, for light, $v = 1$) lead to extreme deflection angles, orders of magnitude larger than observed, and of a very different type. This can be exemplified with the gravitomagnetic equatorial potential \mathcal{A}_ϕ in Eq. (23) of [9], claimed in some literature to flatten the rotation curves (but shown in [9] to be actually sourced by unphysical singularities). We have, using the values in [9] for the galaxy NGC 1560, and the Newtonian potential U in Eq. (15) therein, $|\vec{H}|/|\vec{G}| > Kr^{-7.3/30}$, with $K = 6400 \text{ kpc}^{7.3/30} = 1/C$, thus $|\vec{H}|/|\vec{G}| > 10^3$ throughout the whole galaxy ($R \lesssim 10 \text{ kpc}$). Numerical computation of the ray trajectories yields an equatorial plot resembling that in Fig. 3, with rays hugely deflected in the same direction on both sides of the lens, and not even crossing along the lens-source axis.

B. The Balasin-Grumiller (BG) “galactic” model

The BG solution is described by the metric [5]

$$ds^2 = -(dt - N d\phi)^2 + r^2 d\phi^2 + e^\mu (dr^2 + dz^2); \quad (29)$$

$$N(r, z) = \frac{V_0}{2} \sum_{\pm} \left[\sqrt{(z \pm r_0)^2 + r^2} - \sqrt{(z \pm R)^2 + r^2} \right] + V_0(R - r_0), \quad (30)$$

claimed to describe a galactic dust model in comoving coordinates, with r_0 the radius of the bulge region, and R roughly the radius [6] of the galactic disk in the equatorial plane. It has, however, been recently shown in [11] to actually consist of a dust static with respect to the asymptotic inertial frame (hence totally unsuitable as a galactic model), held in place by unphysical singularities along the symmetry axis, and the claimed flat rotation curves to be but an artifact of an unsuitable choice of reference observers (the zero angular momentum observers—ZAMOs, which undergo circular motions with respect to inertial frames at infinity, due to the artificially large frame-dragging effects created by the singu-

larities). It turns out to be also an archetypal example for Secs. III and IV.

Since $\vec{G} = 0$ and $\vec{J} = 0$ [11], Eqs. (15)–(16) yield $\vec{\nabla} \cdot \vec{H} = 0$, $\vec{\nabla} \times \vec{H} = 0$, and

$$\vec{\nabla} \cdot \vec{G} = -4\pi\rho + \frac{1}{2}\vec{H}^2 = 0. \quad (31)$$

Linearization of this equation leads to the empty space equation $\rho = 0$; hence, the solution has no linear or Newtonian limit, being thus a purely nonlinear solution. In fact, it is an extreme example of the phenomenon discussed in Sec. IV: the repulsive action of the nonlinear contribution $\vec{H}^2/2$ is such that it *cancels out* exactly the attractive gravitational effect of the dust’s energy density (allowing the gravitoelectric field \vec{G} to vanish [11]).

The equation for null geodesics, from Eqs. (2), (10), and (12), becomes here

$$\frac{d^2x^i}{d\lambda^2} + \Gamma(h)_{jl}^i k^j k^l = \nu \vec{k} \times \vec{H} = \nu^2 \vec{v} \times \vec{H}.$$

If one approximates, as done in [5], $\mu \approx \text{const.}$, the space metric h_{ij} becomes flat, $\Gamma(h)_{jl}^i$ become the Christoffel symbols of a cylindrical coordinate system in Euclidean space, and the spacetime an example of a solution where light deflection is solely driven by the gravitomagnetic “force” $\nu^2 \vec{v} \times \vec{H}$. The numerical results, for the parameters suggested in [5] for the Milky Way ($r_0 = 1 \text{ kpc}$, $R = 100 \text{ kpc}$, $V_0 = 220 \text{ km/s}$) and a point light source in the equatorial plane at a distance 1 Gpc from the origin (within the typical order of magnitude of the sources’ distance of observed Einstein rings, e.g. [33, 37]), are plotted in Fig. 3. For a finite light source of radius 20 kpc, the resulting images, obtained with the GYOTO [68] ray-tracing code, are shown in Fig. 4 for different source positions.

They are consistent with the expectation for the gravitomagnetic field as plotted in Fig. 5 of [11], generated by a pair of rods with opposite Newman–Unti–Tamburino (NUT) charges located along the z -axis at $r_0 < z < R$ and $-R < z < -r_0$. In the equatorial plane, $\vec{H}|_{z=0} = |H|\partial_z$ points always in the same direction orthogonal to the plane; hence, light rays passing through opposite sides of the galaxy are deflected in the same direction (the ∂_y direction). The rays do not cross along the line of sight of an observer aligned with the light source and foreground galaxy, resulting in a single image, shown in Fig. 4(b) for an observer at $x_{\mathcal{O}} = -0.1 \text{ Gpc}$; such image is moreover deformed and shifted in the negative y -direction (by a huge angle $\approx 150 \text{ arcsec}$). Observe that, for a spherical lens with $M = 10^{12} M_{\odot}$ (approximately the Milky Way’s mass), this aligned setting would yield instead an Einstein ring with angular radius [26, 27, 69] $\theta_E = \sqrt{4M d_{\text{ls}} / (d_s d_l)} \approx 9 \text{ arcsec}$, where $d_{\text{ls}} = x_s = 1 \text{ Gpc}$ is the distance between the lens and the source (located at $x_1 = 0$), and $d_s = (x_s - x_{\mathcal{O}}) = 1.1 \text{ Gpc}$ and $d_l = -x_{\mathcal{O}} = 0.1 \text{ Gpc}$ are the distances between the observer and, respectively, the source and lens.

Light sources shifted from the optical axis in the negative y -direction yield also a single image, consistent with the fact

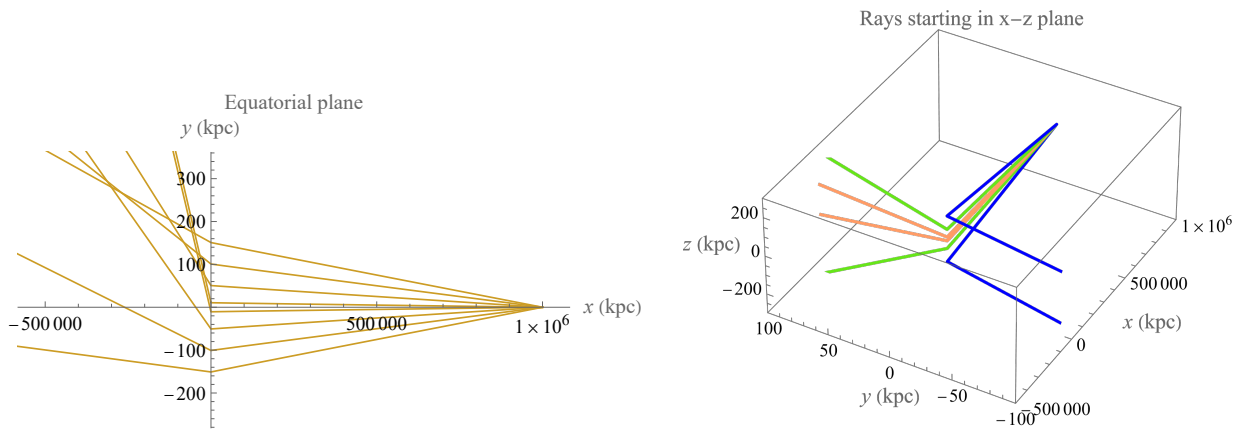


Figure 3. Gravitational light deflection (numerical results) in the Balasin-Grumiller solution for $r_0 = 1$ kpc, $R = 100$ kpc, $V_0 = 220$ km/s, $\mu \approx 1$, and a light source at $(x, y, z) = (10^3 \text{ Mpc}, 0, 0)$. Left panel: in the equatorial plane, light rays through opposite sides of the body are deflected in the same direction. Right panel: light rays starting out in the zOx plane. Each color corresponds to a pair of rays with symmetric angles about the equator; these are made to diverge along the z -direction, and are moreover deflected along the positive y -direction if they approach the z -axis at $|z| < R$, and in the opposite direction at $|z| > R$. This is consistent with the presence of a pair of axial (oppositely charged) NUT rods located at $r_0 < |z| < R$, whose gravitomagnetic field (Fig. 5 of [11]) drives the deflection. Multiple images of the source occur at some points [see Fig. 4(d)], namely on the $y > 0$ side of the equatorial plane, where light rays cross; but no Einstein rings are possible.

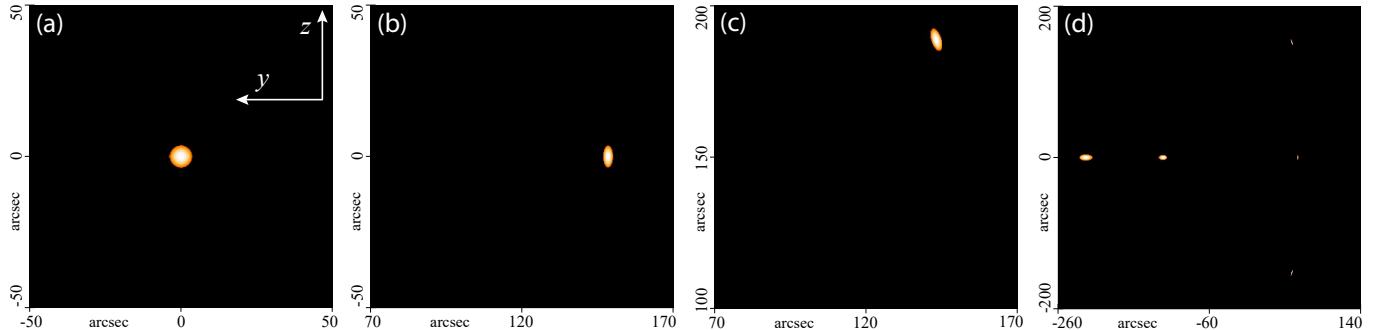


Figure 4. Images corresponding to the setting in Fig. 3, for a spherical light source of radius $R_s = 20$ kpc, at a distance 1.1×10^3 Mpc from the observer, located along the x -axis at $(x_O, y_O, z_O) = (-10^2 \text{ Mpc}, 0, 0)$. Angular coordinates represent altitude (zero in the equatorial plane) and azimuth (zero along the negative x -semi-axis) in the observer’s sky. Panel (a) is the unlensed image of the light source, located at $(x_s, y_s, z_s) = (10^3 \text{ Mpc}, 0, 0)$, in Minkowski spacetime. Panels (b)–(c) are images in the Balasin-Grumiller spacetime. In (b) the source is again located at $(x_s, y_s, z_s) = (10^3 \text{ Mpc}, 0, 0)$ (i.e., observer, lens, and source all aligned along the x -axis); the result is a single image, oblatelly deformed, and shifted in the negative y -direction. Panel (c) is the single image of a source located, in the xOz plane, at $(x_s, y_s, z_s) = (10^3 \text{ Mpc}, 0, 1 \text{ Mpc})$. In panel (d) the source is located in the equatorial plane at $(x_s, y_s, z_s) = (10^3 \text{ Mpc}, 1.64 \text{ Mpc}, 0)$ [i.e., $(r_s, \phi_s, z_s) = (10^3 \text{ Mpc}, 339 \text{ arcsec}, 0)$]. The setting is equivalent to an observer at $(x_O, y_O, z_O) = (-10^5 \text{ kpc}, 164 \text{ kpc}, 0)$ in the left panel of Fig. 3; the result are multiple distorted images of the source. All the images correspond to numerical simulations performed with the GYOTO ray-tracing code [68].

that in the $y < 0$ side of the setting in Fig. 3 light rays do not cross. The same applies to sources shifted along the xOz plane, as shown in Fig. 4(c). Some light rays do cross on the $y > 0$ side of the setting in Fig. 3, leading to multiple images of the source, shown in Fig. 4(d) (for the equivalent situation of an observer along the x -axis and a source displaced in the positive y -direction by the same angle relative to the axis). These images display moreover a huge angular separation [about 290 arcsec in Fig. 4(d)]. Therefore, it is clear that the BG model cannot produce Einstein rings such as those observed in [32, 33]. The lensing effects it generates, besides of a very different type, are moreover of a magnitude much larger than observed.

C. Gravitomagnetic dipole model

In [70] a galactic model based on a so-called “gravitomagnetic dipole” is proposed. It consists of the solution obtained in [71, 72] from a (nonlinear) superposition of two NUT solutions, interpreted as a pair of NUT “objects” of equal masses and equal in magnitude, but opposite, NUT charges. The lengthy expression for the metric is given in Eqs. (1)–(10) of [70]. It depends only on three parameters: the mass M and NUT charge $\pm Q_{\text{NUT}}$ ($\pm \nu$, in the notation of [70, 71]) of each object, and their separation $2k$. For sufficiently large k , the objects are interpreted as a pair of NUT black holes connected by a spinning Misner string [70]. The gravitomagnetic

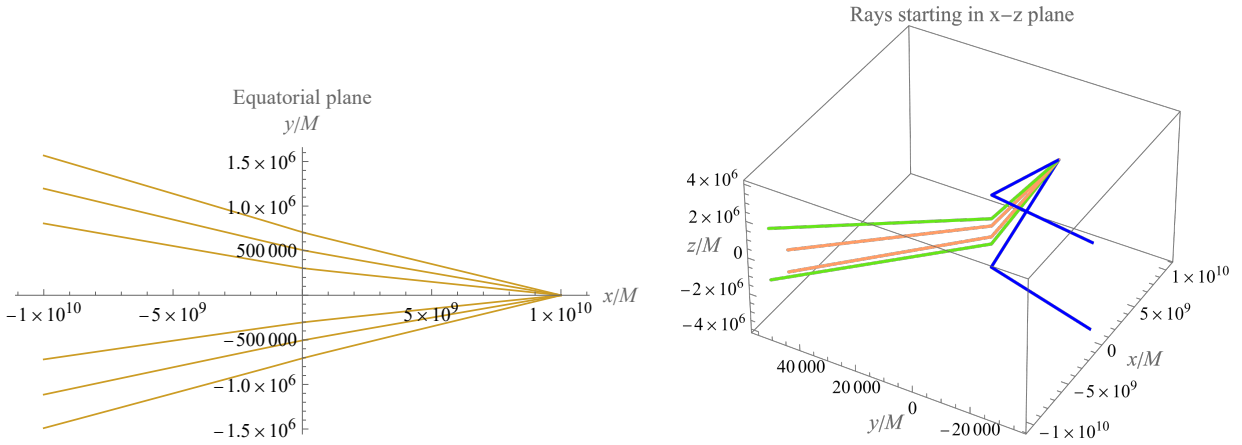


Figure 5. Gravitational light deflection (numerical results) in the gravitomagnetic dipole model, for $Q_{\text{NUT}} = \pm M$, separation $2k = 3.6 \times 10^6 M$, and a light source at a distance $r = 10^{10} M$. No convergence of light rays is produced, which immediately rules out this setting as a viable galactic model. Left panel: rays in the equatorial plane are made to diverge. Right panel: light rays starting out in the zOx plane (each color corresponds to a pair of rays with symmetric angles about the x -axis). They are deflected orthogonally to that plane; along the positive y -direction if they approach the z -axis in the region between the two NUT black holes, $|z| < k$, and in the opposite direction otherwise, as expected from the gravitomagnetic field plotted in Fig. 6.

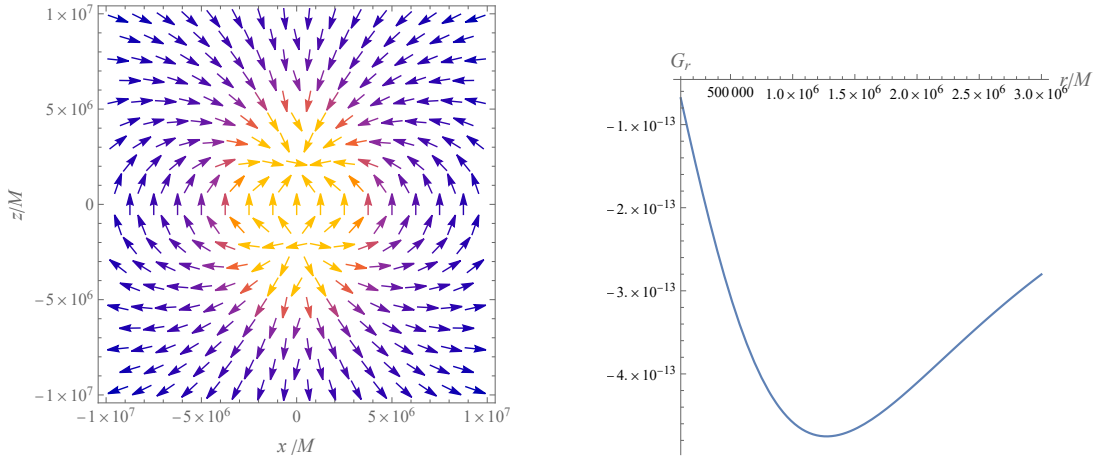


Figure 6. Left panel: x - z plot of the gravitomagnetic field \vec{H} for the gravitomagnetic dipole model with $Q_{\text{NUT}} = \pm M$, and separation $2k = 3.6 \times 10^6 M$; color represents field strength (blue=weak, yellow=strong). Right panel: radial component of the equatorial gravitoelectric field \vec{G}_r , as a function of r . Albeit attractive, $|G_r|$ does not monotonically decrease with r .

field (4) plotted in Fig. 6 is indeed consistent with a pair of opposite gravitomagnetic monopoles (NUT singularities). We choose the values $\nu \simeq M$ and $k = 1.8 \times 10^6 M$ as proposed in Eqs. (82) and (85) of [70], claimed therein⁴ to yield, for $M = 2.6 \times 10^{11} M_\odot$ ($M_\odot \equiv$ solar mass), a nearly flat velocity profile for circular equatorial geodesics approximately

⁴ In [70] a flat velocity curve with $v \approx 8 \times 10^{-4}$ is obtained within the range $4 \times 10^5 < r/M < 1.5 \times 10^6$, corresponding, for $M = 2.6 \times 10^{11} M_\odot$, to $5 \text{ kpc} < r < 19 \text{ kpc}$. This is however actually an artifact of an incorrect approximation made in Eq. (65) of [70]. An exact computation using Eqs. (13) or (14) reveals a curve displaying a much less pronounced flattened region, and in a different range, $1.5 \times 10^6 < r/M < 3.5 \times 10^6$, where it is almost indistinguishable from the Newtonian analogue generated by two point masses separated by a distance $2k$, Eq. (99) of [70]. A detailed account of the circular geodesics in this metric shall be given elsewhere.

matching the observed flat region of the Milky Way rotation curve.

The trajectories of light rays emitted from a light source in the equatorial plane at $r = 10^{10} M$, corresponding (again, for $M = 2.6 \times 10^{11} M_\odot$) to 10^2 Mpc , i.e., roughly 100 times the average distance between nearby galaxies, is plotted in Fig. 5. No convergence of light rays is produced (thus no Einstein rings, nor multiple image of the source); the rays diverge. This completely rules out this model as a viable galactic model.

Light rays starting in the equatorial plane diverge along that plane; the effect, however, is actually not caused by the gravitomagnetic field. It occurs as well when $Q_{\text{NUT}} = 0 \Rightarrow \vec{A} = \vec{H} = 0$ (in which case the setting is held static by the tension of the string). In fact, the plot corresponding to $Q_{\text{NUT}} = 0$ is only slightly changed comparing to the left

panel of Fig. 5, being then symmetric with respect to the x -axis. The effect (which, in appearance, reminds a repulsive scattering) occurs as well for massive particles (i.e., time-like worldlines). Inspection of the radial equation $d^2r/d\tau^2 = -\Gamma_{\alpha\beta}^r U^\alpha U^\beta$ shows that it stems from the weakness of the attractive term $-\Gamma_{00}^r E^2 (g^{00})^2 = e^{-2\Phi} G^r E^2$ (see Footnote 1; here $E \equiv -U_\alpha \partial_t^\alpha = -U_0$ is the particle's energy per unit mass), due to the unusual behavior of the gravitoelectric field \vec{G} , plotted in Fig. 6: although always attractive ($G_r < 0$), its magnitude does not monotonically increase with decreasing r ; in fact, within the region $r/M < 1.5 \times 10^6$ (which includes the flat profile range), $|\vec{G}|$ decreases approaching $r = 0$, with $\lim_{r \rightarrow 0} \vec{G} = 0$. This contrasts with e.g. the situation in the Schwarzschild geometry (where $|G_r|$ monotonically increases until the horizon, where $\lim_{r \rightarrow r_+} G_r = -\infty$), or in Levi-Civita or Lewis-Weyl cylinders [16], and causes the centrifugal term $-\Gamma_{\phi\phi}^r L^2 (g^{\phi\phi})^2 = (1/2) g_{\phi\phi,r} L^2 (g^{\phi\phi})^2 / g_{rr}$ to sharply dominate the scattering (hence the apparent repulsion). Here $L \equiv U_\alpha \partial_\phi^\alpha = U_\phi$ is the test particle's angular momentum per unit mass. The same conclusion can be reached by inspecting the effective potential $V_{\text{eff}}(E, L, r)$ that follows from the equation $U^\alpha U_\alpha = -1 \Leftrightarrow (dr/d\tau)^2 = -2V_{\text{eff}}$, so that $d^2r/d\tau^2 = -dV_{\text{eff}}/dr$.

Light rays starting out in the z_Ox plane are deflected orthogonally to that plane, via the action of the gravitomagnetic field \vec{H} .

It should moreover be noted that (as correctly noticed in [70]) the z -distance $2k = 3.6 \times 10^6 M$ between the NUT black holes is comparable or larger than the galaxy size, which adds to the unrealistic character of the model.

VI. CONCLUSION

We have shown that, in light of the experimentally measured galactic rotation curves and gravitational lensing, general relativity cannot resolve the missing mass problem usually attributed to dark matter, and considering nonlinear corrections only aggravates the problem. In the process we wrote the equations for light propagation in the quasi-Maxwell formalism, and by gravitational lensing ruled out any galactic model (linear or nonlinear) based on gravitomagnetism, as well as the recent ‘‘dipole’’ models (gravitomagnetic or not, linear or not).

Acknowledgments

We thank A. Pollo, E. Malec, P. Mach, and D. Grumiller for correspondence and very useful discussions. We are also indebted to T. Paumard and F. Vincent for generous and crucial help in implementing the GYOTO ray-tracing code, and to the anonymous referee for valuable remarks and suggestions. L.F.C. and J.N. were supported by FCT/Portugal through Projects UIDB/MAT/04459/2020 and UIDP/MAT/04459/2020.

Appendix A: Lensing in the Schwarzschild and Kerr spacetimes

For comparison with the lensing effects of the models in Secs. VB and VC, in order to evince their unphysical character, we present in Figs. 7 and 8 the corresponding ray trajectories and lensed images produced by a Schwarzschild black hole (displaying some essential features common to other compact and spherically symmetric lenses) and, to display the role of the gravitomagnetic field, of a fast spinning Kerr black hole.

In the Schwarzschild case, the deflection is the same for rays starting at equal (in magnitude) angles relative to the axis connecting the source and the black hole; this leads to perfect Einstein rings as viewed by observers along this axis [20, 29, 69, 73, 74] (‘‘optical axis’’; here, the x -axis). Namely, the image of an idealized point source is a (infinitely bright) circle; for a real, finite source, the image is a ring of finite width [27, 28], exemplified in the simulation in Fig. 8(b).

In the Kerr spacetime, the lens is not spherically symmetric; consequently, for an idealized point source, the Einstein ring does not form [20, 50–52]. The primary caustic surface [75] behind the black hole no longer degenerates into the optical axis, having instead a finite astroid section (see e.g. Figs. 2–3 in [50]), and the image of point sources (inside or outside it) are a finite set of points (not some 1D contour) [50, 52, 75]. For finite sources, however, rings can still form, when the source is large enough to cover to whole caustic section [27, 28]. In this case, the impact of the black hole's spin is the following. The gravitomagnetic field (which is approximately dipole-like, as depicted in Fig. 2) causes the deflection angles of equatorial light rays through opposite sides of the black hole to differ (left panel of Fig. 7). Hence, rays starting at equal but opposite angles relative to the x -axis will not cross along that axis; conversely, those that do, arrive at different angles. On light rays with initial direction along the z_Ox plane, the gravitomagnetic field causes a deflection along the y -direction, causing them not to cross along the x -axis (besides not contributing to their convergence which, as in the Schwarzschild case, is along the z -direction). Consequently, the caustic behind the black hole is transversely displaced (in the y -direction) from the optical axis, cf. e.g. Fig. 2 in [50]. As a result, the image of a finite source along the optical axis will in general be two arcs, as exemplified in the simulation in Fig. 8(c); if the source extends until the caustic location (and covering it) the arcs will close into a deformed ring, weakened at the poles, and slightly shifted in the negative y -direction. This is similar to the situation in a Schwarzschild lens of the same mass, but for a source displaced from the optical axis. For a source centered at the center of the caustic section, and fully covering it, the image will be an almost perfect Einstein ring similar to that produced by a Schwarzschild lens of the same mass for a source along the optical axis, only shifted along the y -direction, as shown in Fig. 8(d). The ring's angular diameter (hence the lens power), in particular, is the same. (Such a ring is also slightly deformed [51]; the effect is however almost unnoticeable in the simulations performed.) It is thus clear that the gravitomagnetic field does not enhance the optical effect generating Einstein rings. Indeed, for sources

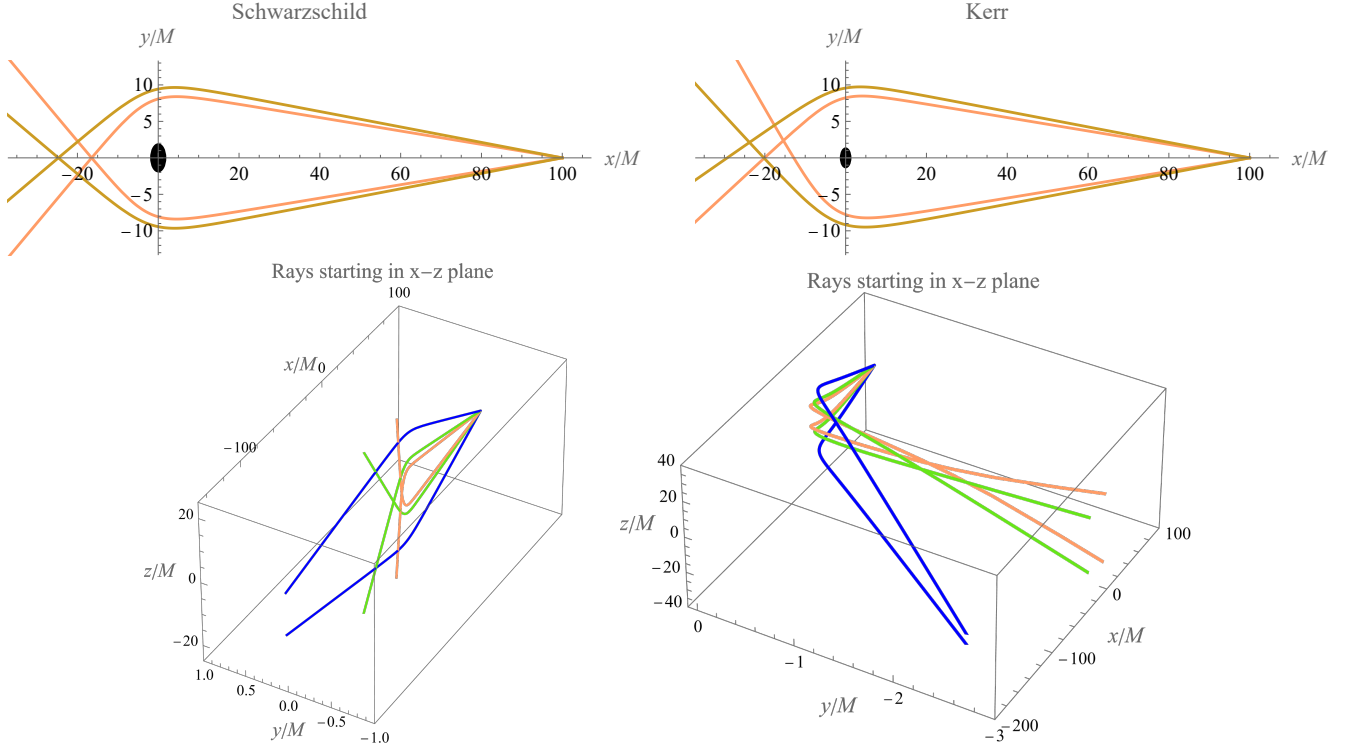


Figure 7. Gravitational light deflection (numerical results) in the Schwarzschild and in a Kerr spacetime with rotation parameter $a = S/M = 0.9$. The source is at a distance $r = 100M$. First row: equatorial plane; second row: light rays starting out in the zOx plane. Each color corresponds to a pair of rays with symmetric angles about the x -axis. In the Schwarzschild case, the deflection is the same for rays starting at equal (in magnitude) angles relative to the x -axis connecting the source and the black hole; this leads to perfectly circular Einstein rings as viewed by observers along the x -axis [Fig. 8 (b)]. In the Kerr spacetime, the deflection of equatorial light rays through opposite sides of the black hole differs; rays starting at equal (in magnitude) angles will not cross along the x -axis; and those that do cross along the x -axis arrive at different angles. Light rays with initial direction along the zOx plane suffer (in addition to the convergence along the z -axis), a deflection along the y -direction. These gravitomagnetic effects do not enhance the convergence of light rays for observers along the x -axis, instead mimicking a non-aligned Schwarzschild lens, as shown in Figs. 8 (c)-(d).

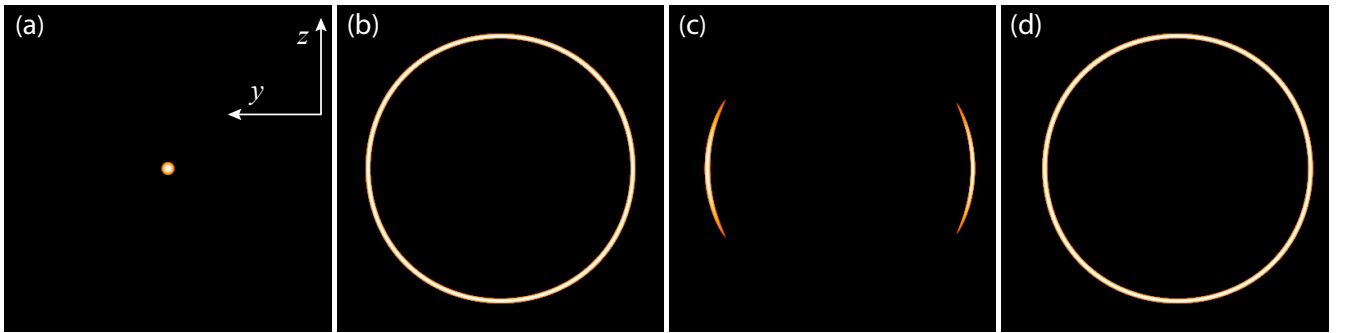


Figure 8. Images produced by the settings in Fig. 7, for a spherical light source of radius $R_s = 3M$. Panel (a) is the unlensed image of the light source in Minkowski spacetime. Panel (b) is the image of the source when placed behind a Schwarzschild black hole (of mass M) along the optical axis (i.e., light source, black hole, and observer all aligned along the x -axis). The source is located at $(x_s, y_s, z_s) = (100M, 0, 0)$, and the observer at $(x_o, y_o, z_o) = (-20M, 0, 0)$; the black hole is at the origin. The resulting image is a perfect Einstein ring. Panel (c): image produced by a similarly aligned setting for a Kerr black hole with $a = 0.9$; it results in a pair of arcs. Panel (d): for the same Kerr black hole and observer position, the light source is now placed at the center of the primary caustic $(x_s, y_s, z_s) \approx (100M, -6M, 0)$, which is transversely displaced [52] from the optical axis by $\Delta y \approx -6M$. (The caustic section is therein about $0.1M$ wide, cf. Eq. (19) of [52], much smaller than the source's diameter). The image is an Einstein ring almost identical to panel (b), only transversely shifted in the y -direction. All the images correspond to numerical simulations performed with the GYOTO ray-tracing code [68].

large enough for the ring to still form, unless their displacement from the optical axis can be verified by an independent

method, one cannot, based only on the observed Einstein rings, distinguish a spinning from a non-spinning black hole with the same mass [66, 67].

-
- [1] M. L. Ruggiero, A. Ortolan, and C. C. Speake, “Galactic dynamics in general relativity: the role of gravitomagnetism,” *Class. Quant. Grav.* **39** no. 22, (2022) 225015, [arXiv:2112.08290](#).
- [2] D. Astesiano and M. L. Ruggiero, “Can general relativity play a role in galactic dynamics?” *Phys. Rev. D* **106** no. 12, (2022) L121501, [arXiv:2211.11815](#).
- [3] F. I. Cooperstock and S. Tieu, “General relativity resolves galactic rotation without exotic dark matter,” [arXiv:astro-ph/0507619](#).
- [4] J. D. Carrick and F. I. Cooperstock, “General relativistic dynamics applied to the rotation curves of galaxies,” *Astrophys. Space Sci.* **337** (2012) 321–329, [arXiv:1101.3224](#).
- [5] H. Balasin and D. Grumiller, “Non-Newtonian behavior in weak field general relativity for extended rotating sources,” *Int. J. Mod. Phys. D* **17** (2008) 475–488, [arXiv:astro-ph/0602519](#).
- [6] M. Crosta, M. Giammaria, M. G. Lattanzi, and E. Poggio, “On testing CDM and geometry-driven Milky Way rotation curve models with Gaia DR2,” *Mon. Not. Roy. Astron. Soc.* **496** no. 2, (2020) 2107–2122, [arXiv:1810.04445](#).
- [7] D. Astesiano and M. L. Ruggiero, “Galactic dark matter effects from purely geometrical aspects of general relativity,” *Phys. Rev. D* **106** no. 4, (2022) 044061, [arXiv:2205.03091](#).
- [8] L. Ciotti, “On the Rotation Curve of Disk Galaxies in General Relativity,” *Astrophys. J.* **936** no. 2, (2022) 180, [arXiv:2207.09736](#).
- [9] A. N. Lasenby, M. P. Hobson, and W. E. V. Barker, “Gravitomagnetism and galaxy rotation curves: a cautionary tale,” *Class. Quant. Grav.* **40** (2023) 215014, [arXiv:2303.06115](#).
- [10] K. Glampedakis and D. I. Jones, “Pitfalls in applying gravitomagnetism to galactic rotation curve modelling,” *Class. Quant. Grav.* **40** (2023) 147001, [arXiv:2303.16679](#).
- [11] L. F. O. Costa, J. Natário, F. Frutos-Alfaro, and M. Soffel, “Reference frames in general relativity and the galactic rotation curves,” *Phys. Rev. D* **108** (2023) 044056, [arXiv:2303.17516](#).
- [12] L. D. Landau and E. M. Lifshitz, *The classical theory of fields; 4th ed.*, vol. 2 of *Course of theoretical physics*. Butterworth-Heinemann, Oxford, UK, 1975. Trans. from the Russian.
- [13] D. Lynden-Bell and M. Nouri-Zonoz, “Classical monopoles: Newton, nut space, gravomagnetic lensing, and atomic spectra,” *Rev. Mod. Phys.* **70** (Apr, 1998) 427–445.
- [14] J. Natário, “Quasi-Maxwell interpretation of the spin-curvature coupling,” *General Relativity and Gravitation* **39** no. 9, (Sep, 2007) 1477–1487.
- [15] L. F. O. Costa and J. Natário, “Gravito-electromagnetic analogies,” *General Relativity and Gravitation* **46** no. 10, (2014) 1792, [arXiv:1207.0465](#).
- [16] L. F. O. Costa, J. Natário, and N. O. Santos, “Gravitomagnetism in the Lewis cylindrical metrics,” *Class. Quant. Grav.* **38** no. 5, (2021) 055003, [arXiv:1912.09407](#).
- [17] R. Gharechahi, J. Koohbor, and M. Nouri-Zonoz, “General relativistic analogs of Poisson’s equation and gravitational binding energy,” *Phys. Rev. D* **99** (2019) 084046.
- [18] R. T. Jantzen, P. Carini, and D. Bini, “The Many faces of gravitoelectromagnetism,” *Annals Phys.* **215** (1992) 1–50, [arXiv:gr-qc/0106043](#).
- [19] D. Bini, P. Carini, and R. T. Jantzen, “The Intrinsic derivative and centrifugal forces in general relativity. I. Theoretical foundations,” *Int. J. Mod. Phys. D* **6** (1997) 1–38, [arXiv:gr-qc/0106013](#).
- [20] V. Perlick, “Gravitational lensing from a spacetime perspective,” *Living Reviews in Relativity* **7** (2004) 9.
- [21] V. J. Bolos, “Intrinsic definitions of ‘relative velocity’ in general relativity,” *Commun. Math. Phys.* **273** (2007) 217–236, [arXiv:gr-qc/0506032](#).
- [22] S. Datta and S. Mukherjee, “Possible connection between the reflection symmetry and existence of equatorial circular orbit,” *Phys. Rev. D* **103** no. 10, (2021) 104032, [arXiv:2010.12387](#).
- [23] S. Carroll, *Spacetime and Geometry: An Introduction to General Relativity*. Addison Wesley, 2004.
- [24] H. Stephani, D. Kramer, M. A. H. MacCallum, C. Hoenselaers, and E. Herlt, *Exact solutions of Einstein’s field equations*. Cambridge University Press, 2004.
- [25] A. Einstein, “Lens-like action of a star by the deviation of light in the gravitational field,” *Science* **84** no. 2188, (1936) 506–507.
- [26] J. Pinochet and M. V. S. Jan, “Einstein ring: weighing a star with light,” *Physics Education* **53** no. 5, (Jun, 2018) 055003, [arXiv:1801.00001](#).
- [27] A. Petters, H. Levine, and J. Wambsganss, *Singularity Theory and Gravitational Lensing*. Progress in Mathematical Physics. Birkhäuser Boston, 2001.
- [28] P. Schneider, J. Ehlers, and E. Falco, *Gravitational Lenses*. Astronomy and Astrophysics Library. Springer, 1999.
- [29] K. S. Virbhadra, “Relativistic images of Schwarzschild black hole lensing,” *Phys. Rev. D* **79** (2009) 083004, [arXiv:0810.2109 \[gr-qc\]](#).
- [30] P. Salucci, “The distribution of dark matter in galaxies,” *Astron. Astrophys. Rev.* **27** no. 1, (2019) 2, [arXiv:1811.08843](#).
- [31] C. S. Kochanek, C. R. Keeton, and B. A. McLeod, “The importance of Einstein rings,” *Astrophys. J.* **547** (2001) 50, [arXiv:astro-ph/0006116](#).
- [32] L. J. King *et al.*, “A Complete infrared Einstein ring in the gravitational lens system B1938+666,” *Mon. Not. Roy. Astron. Soc.* **295** (1998) L41, [arXiv:astro-ph/9710171](#).
- [33] D. J. Lagattuta, S. Vegetti, C. D. Fassnacht, M. W. Auger, L. V. E. Koopmans, and J. P. McKean, “SHARP - I. A high-resolution multiband view of the infrared Einstein ring of JVAS B1938+666,” *Mon. Not. Roy. Astron. Soc.* **424** no. 4, (2012) 2800–2810, [arXiv:1206.1681](#).
- [34] V. Belokurov *et al.*, “The Cosmic Horseshoe: Discovery of an Einstein Ring around a Giant Luminous Red Galaxy,” *Astrophys. J. Lett.* **671** (2007) L9, [arXiv:0706.2326 \[astro-ph\]](#).

- [35] C. Spiniello, L. V. E. Koopmans, S. C. Trager, O. Czoske, and T. Treu, “The X-Shooter Lens Survey - I. Dark matter domination and a Salpeter-type initial mass function in a massive early-type galaxy,” *Monthly Notices of the Royal Astronomical Society* **417** no. 4, (2011) 3000–3009, [arXiv:1103.4773](#).
- [36] F. Bellagamba, N. Tessore, and R. B. Metcalf, “Zooming into the Cosmic Horseshoe: new insights on the lens profile and the source shape,” *Mon. Not. Roy. Astron. Soc.* **464** no. 4, (2017) 4823–4834, [arXiv:1610.06003](#).
- [37] S. Schuldt, G. Chirivì, S. H. Suyu, A. Yıldırım, A. Sonnenfeld, A. Halkola, and G. F. Lewis, “Inner dark matter distribution of the Cosmic Horseshoe (J1148+1930) with gravitational lensing and dynamics,” *Astronomy & Astrophysics* **631** (2019) A40, [arXiv:1901.02896](#).
- [38] J. Cheng, M. P. Wiesner, E.-H. Peng, W. Cui, J. R. Peterson, and G. Li, “Adaptive Grid Lens Modeling of the Cosmic Horseshoe Using Hubble Space Telescope Imaging,” *Astrophys. J.* **872** no. 2, (Feb., 2019) 185.
- [39] A. Durkalec, A. Pollo, and U. Abbas, “Halo Asymmetry in the Modeling of Galaxy Clustering,” *Astrophys. J.* **966** no. 1, (2024) 73, [arXiv:2404.05030](#).
- [40] A. Amruth, T. Broadhurst, J. Lim, M. Oguri, G. F. Smoot, J. M. Diego, E. Leung, R. Emami, J. Li, T. Chiueh, H.-Y. Schive, M. C. H. Yeung, and S. K. Li, “Einstein rings modulated by wavelike dark matter from anomalies in gravitationally lensed images,” *Nature Astronomy* **7** (2023) 736–747.
- [41] T. Ono, A. Ishihara, and H. Asada, “Gravitomagnetic bending angle of light with finite-distance corrections in stationary axisymmetric spacetimes,” *Phys. Rev. D* **96** no. 10, (2017) 104037, [arXiv:1704.05615](#).
- [42] M. Galoppo, S. L. Cacciatori, V. Gorini, and M. Mazza, “Equatorial Lensing in the Balasin-Grumiller Galaxy Model,” [arXiv:2212.10290 \[gr-qc\]](#).
- [43] A. Ishihara, Y. Suzuki, T. Ono, T. Kitamura, and H. Asada, “Gravitational bending angle of light for finite distance and the Gauss-Bonnet theorem,” *Phys. Rev. D* **94** no. 8, (2016) 084015, [arXiv:1604.08308](#).
- [44] G. W. Gibbons and M. C. Werner, “Applications of the Gauss-Bonnet theorem to gravitational lensing,” *Classical and Quantum Gravity* **25** no. 23, (2008) 235009.
- [45] K. Jusufi, A. Övgün, J. Saavedra, Y. Vásquez, and P. A. González, “Deflection of light by rotating regular black holes using the Gauss-Bonnet theorem,” *Phys. Rev. D* **97** no. 12, (2018) 124024, [arXiv:1804.00643](#).
- [46] M. Halla and V. Perlick, “Application of the Gauss–Bonnet theorem to lensing in the NUT metric,” *Gen. Rel. Grav.* **52** no. 11, (2020) 112, [arXiv:2008.10093](#). [Erratum: *Gen.Rel.Grav.* 53, 68 (2021)].
- [47] F. C. Sánchez, A. A. Roque, B. Rodríguez, and J. Chagoya, “Total light bending in non-asymptotically flat black hole spacetimes,” *Class. Quant. Grav.* **41** (2024) 015019, [arXiv:2306.12488](#).
- [48] W. Klingenberg, *A Course in Differential Geometry*. Graduate texts in mathematics. Springer-Verlag, 1978.
- [49] L. Godinho and J. Natário, *An Introduction to Riemannian Geometry: With Applications to Mechanics and Relativity*. Universitext. Springer International Publishing, 2014.
- [50] K. P. Rauch and R. D. Blandford, “Optical Caustics in a Kerr Spacetime and the Origin of Rapid X-Ray Variability in Active Galactic Nuclei,” *ApJ* **421** (Jan., 1994) 46.
- [51] V. Bozza, “Quasiequatorial gravitational lensing by spinning black holes in the strong field limit,” *Phys. Rev. D* **67** (2003) 103006, [arXiv:gr-qc/0210109](#).
- [52] M. Sereno and F. De Luca, “Primary caustics and critical points behind a Kerr black hole,” *Phys. Rev. D* **78** (2008) 023008, [arXiv:0710.5923](#).
- [53] M. Sereno, “Gravitational lensing by stars with angular momentum,” *Mon. Not. Roy. Astron. Soc.* **344** (2003) 942, [arXiv:astro-ph/0307243](#).
- [54] T. Damour, M. Soffel, and C. Xu, “General relativistic celestial mechanics. 1. Method and definition of reference systems,” *Phys. Rev. D* **43** (1991) 3273–3307.
- [55] M. Soffel, “Standard relativistic reference systems and the IAU framework,” in *Relativity in Fundamental Astronomy: Dynamics, Reference Frames, and Data Analysis*, S. A. Klioner, P. K. Seidelmann, and M. H. Soffel, eds., vol. 261, pp. 1–6. Jan., 2010.
- [56] J. D. Kaplan, D. A. Nichols, and K. S. Thorne, “Post-Newtonian approximation in Maxwell-like form,” *Phys. Rev. D* **80** (2009) 124014, [arXiv:0808.2510](#).
- [57] M. Soffel, S. Klioner, J. Muller, and L. Biskupek, “Gravitomagnetism and lunar laser ranging,” *Phys. Rev. D* **78** (2008) 024033.
- [58] E. Poisson and C. M. Will, *Gravity: Newtonian, Post-Newtonian, Relativistic*. Cambridge University Press, Cambridge, UK, 2014.
- [59] P. Mach and E. Malec, “General-relativistic rotation laws in rotating fluid bodies,” *Phys. Rev. D* **91** no. 12, (2015) 124053, [arXiv:1501.04539](#).
- [60] J. Karkowski, P. Mach, E. Malec, M. Pirog, and N. Xie, “Rotating systems, universal features in dragging and ant dragging effects, and bounds of angular momentum,” *Phys. Rev. D* **94** no. 12, (2016) 124041, [arXiv:1609.06586](#).
- [61] H. Stephani, *Relativity: An Introduction to Special and General Relativity*. Cambridge University Press, 3 ed., 2004.
- [62] J. Ibáñez, “Gravitational lenses with angular momentum,” *Astronomy & Astrophysics* **124** no. 2, (1983) 175–180.
- [63] B. M. Schaefer and M. Bartelmann, “Weak lensing in the second post-Newtonian approximation: Gravitomagnetic potentials and the integrated Sachs-Wolfe effect,” *Mon. Not. Roy. Astron. Soc.* **369** (2006) 425–440, [arXiv:astro-ph/0502208](#).
- [64] I. Ciufolini and J. A. Wheeler, *Gravitation and Inertia*. Princeton Series in Physics, Princeton, NJ, 1995.
- [65] J. Ibáñez and J. Martín, “Gravitational scattering of spinning particles: Linear approximation,” *Phys. Rev. D* **26** (1982) 384–389.
- [66] M. Sereno and F. De Luca, “Analytical Kerr black hole lensing in the weak deflection limit,” *Phys. Rev. D* **74** (2006) 123009, [arXiv:astro-ph/0609435](#).
- [67] H. Asada and M. Kasai, “Can we see a rotating gravitational lens?,” *Prog. Theor. Phys.* **104** (2000) 95, [arXiv:astro-ph/0006157](#).
- [68] F. H. Vincent, T. Paumard, E. Gourgoulhon, and G. Perrin, “GYOTO: a new general relativistic ray-tracing code,” *Class. Quant. Grav.* **28** (2011) 225011, [arXiv:1109.4769](#).
- [69] K. S. Virbhadra and G. F. R. Ellis, “Schwarzschild black hole lensing,” *Phys. Rev. D* **62** (2000) 084003, [arXiv:astro-ph/9904193](#).
- [70] J. Govaerts, “The gravito-electromagnetic approximation to the gravimagnetic dipole and its velocity rotation curve,” *Class. Quant. Grav.* **40** no. 8, (2023) 085010, [arXiv:2303.01386](#).
- [71] G. Clément, “The gravimagnetic dipole,” *Class. Quant. Grav.* **38** (2021) 075003, [arXiv:2010.14473](#).
- [72] V. S. Manko, E. D. Rodchenko, E. Ruiz, and M. B. Sadovnikova, “Formation of a Kerr black hole from two

- stringy NUT objects,” *Moscow Univ. Phys. Bull.* **64** (2009) 359, [arXiv:0901.3168](#).
- [73] O. James, E. von Tunzelmann, P. Franklin, and K. S. Thorne, “Gravitational lensing by spinning black holes in astrophysics, and in the movie interstellar,” *Classical and Quantum Gravity* **32** no. 6, (Feb, 2015) 065001.
- [74] G. S. Bisnovatyi-Kogan and O. Y. Tsupko, “Strong Gravitational Lensing by Schwarzschild Black Holes,” *Astrophysics* **51** (2008) 99–111, [arXiv:0803.2468](#).
- [75] V. Bozza, “Optical caustics of Kerr spacetime: The Full structure,” *Phys. Rev. D* **78** (2008) 063014, [arXiv:0806.4102](#).